

10 Mp APS Format Color Full-Frame CCD Image Sensor

Eric J. Meisenzahl*, William F. DesJardin, Robert Kaser, John P. Shepherd; Eastman Kodak Company; Rochester, NY/USA

Abstract

This paper describes the design and performance of a new APS-sized CCD image sensor using an advanced 6.8 μm pixel. The pixels are arranged in a 3970 (H) \times 2646 (V) format to support a 3:2 aspect ratio. Unique to this pixel is the implementation of an under-the-field oxide (UFOX) lateral overflow drain (LOD) and thin light-shield technology that provides higher charge capacity, higher quantum efficiency, and wider incident angle response. Each pixel contains a microlens to improve sensitivity and a dual-split HCCD shift register with high sensitivity amplifiers, which are used to increase frame rate while lowering noise.

Introduction

APS class cameras require high performance image sensors with ever demanding requirements. Each new generation of image sensor requires potentially more pixels, improved pixel performance, or new operating features. Using technology that was originally developed for the medium format camera market [1], the pixel performance and frame rate of an existing 10 Mp, 6.8 μm image sensor was improved.

Design

Figure 1 shows the 10 Mp full-frame image sensor block diagram. It consists of a vertical CCD (VCCD) array of pixels that cover a photoactive area of 27 \times 18 mm. A dual-split horizontal CCD (HCCD) register accepts each line from the VCCD and shifts pixels to two high-sensitivity output nodes in a serial fashion. This arrangement reduces the frame readout time by approximately one half compared to the older, 10 Mp single output device. The design supports a data rate of 48 Mpixels/s and produces a maximum frame rate of 3.7 fps. The device is housed in a 60-pin PGA ceramic package with 0.100 in. pin spacing.

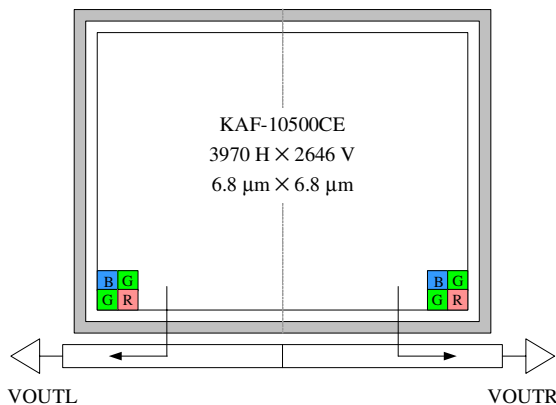


Figure 1. 10 Mp image sensor block diagram.

Pixel

Each pixel consists of single polysilicon and single ITO gates, as shown in Fig. 2. Barrier regions (B1, B2) are formed within the silicon substrate to confine the signal during exposure and readout. In addition, a (B3) barrier region is formed to skim off excess signal in the event exposure in the pixel exceeds its capacity. The LOD provides the means to drain any excessive signal off-chip, and channel stops (Chst) serve to isolate pixels horizontally. Figure 3 shows an electrostatic model of the potentials developed during operation. The photosensitive fill factor of this pixel is 69%, resulting from the fact that the LOD region does not collect signal. To increase sensitivity, the pixel is designed with a reduced aperture light shield and overlying microlens. The aperture opening is first positioned to expose only the ITO gate, which has superior light transmission characteristics compared to the polysilicon gate [2]. The microlens position, height, and shape are then designed such that light is directed away from the insensitive LOD region, and less transmissive polysilicon gate, and focused into the center of the aperture opening. Between the microlens and light shield, each pixel is selectively covered with a red, green, or blue color filter material (CFA) in a Bayer [3] configuration to produce color images. With this structure, the effective photosensitive fill factor is increased to 78%.

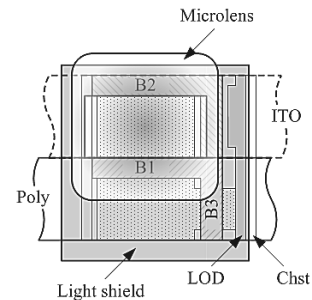


Figure 2. Top view sketch of 6.8 μm pixel design.

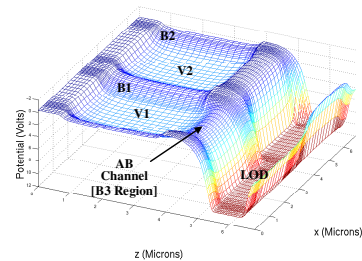


Figure 3. 6.8 μm pixel channel potential model. V1 represents the polysilicon gate electrode and V2 is the ITO electrode.

UFOX LOD [4]

To improve charge capacity, the LOD width is reduced to enlarge the area used to collect signal. In order to maintain the same antiblooming performance, it becomes necessary to decrease the resistance of the drain by increasing the dose of the implant. The problem with this approach in the conventional LOD structure, shown in Fig. 4, is that a gate-dependent breakdown occurs at a lower voltage as the LOD implant is increased. The source of the breakdown has been identified as band-band tunneling caused by high electric fields at the silicon-to-silicon dioxide interface. To alleviate this problem, the LOD implant is, instead, formed underneath the thick field oxide similar in nature to the channel stop formation, as shown in Fig. 5. This shifts the position and magnitude of the maximum electric field region under the field oxide where the overlying gate electrodes have almost no influence. The UFOX LOD, therefore, enables the use of higher implant doses without the breakdown problem, and the LOD width can be reduced without compromising antiblooming protection. More significant is the fact that, with a smaller LOD width, the charge capacity and quantum efficiency of the pixel is increased because of a higher fraction of charge collection area. Last, because more of the gate area is placed over a thick (field) oxide region, the clock capacitance is reduced, resulting in improved line rates and lower power dissipation.

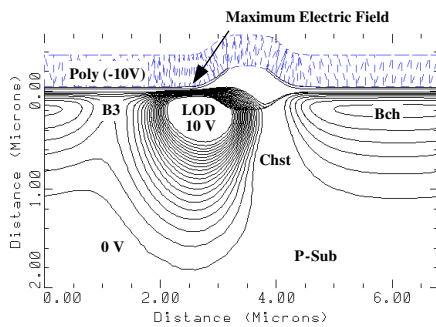


Figure 4. Electrostatic model of conventional LOD. The view shown is the horizontal cross-section through the B3 region of Fig. 2.

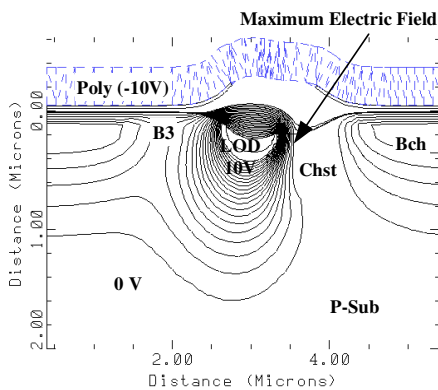


Figure 5. Electrostatic model of UFOX LOD.

Thin Light Shield [5]

Common among current KAF-series image sensors is a metalization process that uses a bilayer of thick aluminum (Al) on top of a thinner TiW film. The two films are deposited in sequence and subsequently patterned and etched as one. This bilayer stack is used for routing clock and bias lines to gates and drains as well as for forming the light shield in the array of pixels. The pixel light shield is used in two ways. First, pixels around the periphery of the device are completely covered with the light shield in order to establish a good dark reference that tracks with temperature, and, secondly, the light shield is placed around the border of photo-active pixels in order to reduce color crosstalk between adjacent pixels. The thin light shield process is an idea that simply removes the aluminum only in areas where photosensitive pixels are to be defined. Holes in the remaining thin TiW layer are then etched to form apertures. This leaves the TiW film to provide color separation while the rest of the device remains as an Al/TiW stack. The optical density that a TiW-only film exhibits is about 3.0. This optical density is acceptable in photosensitive pixels but not in the dark reference pixels. Hence, the aluminum is retained over dark pixels. Using the thin light shield technology, the topography of the pixel is improved and the angle response is extended as light is more easily focused through the aperture opening, as illustrated in the SEM cross-sections of Figs. 6 and 7.

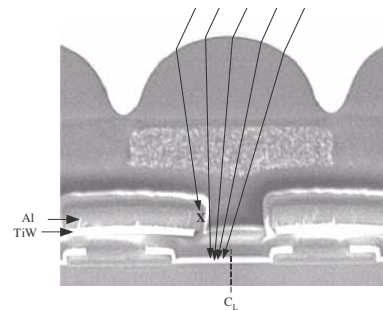


Figure 6. SEM vertical cross-section of older 6.8 μm pixel with standard Al/TiW light shield process. Sketches of light rays are used to illustrate how the light is directed through the light shield aperture opening. When the rays enter at an angle, the focused ray bundle is translated away from the center of the aperture opening (C_L) and one of the light rays (X) hits the opaque light shield and cannot be collected in the pixel, resulting in a loss of signal.

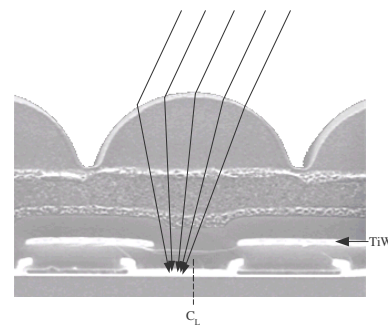


Figure 7. SEM vertical cross-section of new 10 Mp, 6.8 μm pixel device with TiW-only light shield process. Using similar illustrations of light ray sketches as in Fig. 6, note how it is possible to accept a wider range of incident light angles without a loss in signal.

Optical Measurements

Quantum efficiency has been measured on the 10 Mp device and is compared against previous work. Referring to Fig. 8, peak response values achieved are 35%, 42%, and 38%, for red, green, and blue, respectively. This exceeds the values achieved from the older 10 Mp, 6.8 μm microlens design where red, green, and blue QE was measured at 30%, 34%, and 31%, respectively, and can be attributed to a larger aperture size (enabled by UFOX LOD) and reduced CFA layer thicknesses. The saturation-based ISO is reduced from 92 (older 6.8 μm pixel) to 85 (new 6.8 μm pixel) where the increase in QE and responsivity are outweighed compared to the increase in charge capacity. Noise-limited exposure index of the new 6.8 μm pixel would be higher.

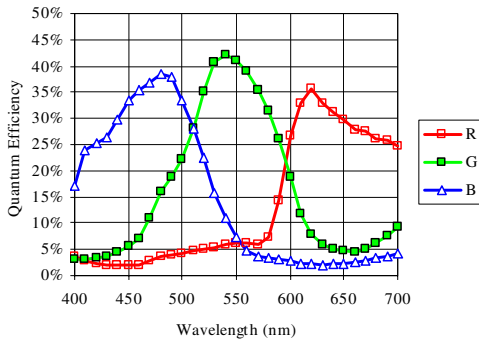


Figure 8. Device quantum efficiency performance.

The (green) pixel responses to incident light angles are shown in Fig. 9. This measurement is made along the vertical (short or worst case) dimension of the chip under white light conditions. White light conditions are defined as the illumination required to balance the output of red, green, and blue pixels at 0° incident angles. The angle response is found to be $\pm 17^\circ$ @ 80% roll-off which is significantly improved over previous work ($\pm 12^\circ$).

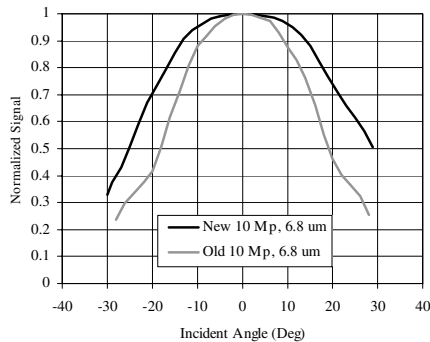


Figure 9. Vertical angle response in comparison to older 10 Mp device.

Electrical Measurements

Compared to the previous 6.8 μm pixel performance, the charge capacity has increased from 40 ke- to 66 ke-, and the noise has been reduced from 17 e- rms to 15 e- rms. The noise reduction is largely the result of improving the output-referred charge-to-voltage gain from 17.5 $\mu\text{V}/\text{e-}$ to 24.5 $\mu\text{V}/\text{e-}$. Dynamic range of the

new pixel, therefore, is 72.9 dB—an increase of 5.7 dB over the previous 6.8 μm pixel design.

Conclusion

The design and performance of a new 10Mp CCD imaging device has been described. This device incorporates UFOX LOD and thin light shield technologies that enable increased charge capacity, higher quantum efficiency, and improved angle response. A summary comparison of other key performance parameters is shown below.

Performance Summary:

Parameter	Symbol	New 10 Mp	Old 10 Mp	Unit
Pixel Size	P	6.8	6.8	$\mu\text{m Sq}$
Charge Capacity	N_{sat}	66	40	ke-
Output Sensitivity	S	24.5	17.5	$\mu\text{V}/\text{e-}$
Noise	N_e	15	17	e- rms
Dynamic Range	DR	72.9	67.4	dB
Quantum Efficiency	η_B, η_G, η_R	38,42,35	31,34,30	% Peak
Angle Response	AR	± 17	± 12	Deg @ 80%
Antiblooming	X_{AB}	>1000	>1000	x Esat
Dark Current	J_d	2	2	pA/cm^2 @ 25°C
Base ISO (Green)	ISO	85	92	3200 °K + IR
Responsivity	R_B, R_G, R_R	39,70,59	30,47,47	ke-/lux-sec
Frame Rate	FR	3.7	2.1	fps

Acknowledgments

The authors thank the members of the Image Sensor Solutions Division at Eastman Kodak Company for the process development, fabrication, packaging, and testing of these sensors.

References

- [1] E.J. Meisenzahl*, E.K. Banghart, D.N. Nichols, J.P. Shepherd, E.G. Stevens, and K.Y. Wong, "31 Mp and 39 Mp Full-Frame CCD Image Sensors with Improved Charge Capacity and Angle Response," SPIE Electronic Imaging Conference, 2006.
- [2] D.M. Brown, M. Ghezzi, and M. Garfinkel, "Transparent Metal Oxide Electrode CID Imager Array," ISSCC Dig. Tech. Papers, pp. 34–35, February 1975.
- [3] B.E. Bayer, U.S. Patent 3,971,065, July 20, 1976.
- [4] E.K. Banghart, E.G. Stevens, H.Q. Doan, J.P. Shepherd, and E.J. Meisenzahl, "An LOD with Improved Breakdown Voltage in Full-Frame CCD Devices," SPIE Electronic Imaging Conference, 2005.
- [5] E.G. Stevens, E.K. Banghart, H.Q. Doan, E.J. Meisenzahl, H. Murata, D.N. Nichols, and J.P. Shepherd, "8.3 MP, 4/3" Full-Frame CCD with Scaled LOD and Micro Optics," IEEE CCD & AIS Workshop, Japan, 2005.

Author Biography

Eric Meisenzahl received his B,S,E,E, from Clarkson University and his M.S.E.E. from Rochester Institute of Technology. He joined Eastman Kodak Company in 1983 and has since been involved in the development of image sensors, primarily in the field of CCD test and characterization. His current assignment is to provide design support for the new generation of color full-frame CCDs for professional photographic markets.